UMT PRESS

Journal of Sustainability Science and Management
Journal Homepage: https://jssm.umt.edu.my
eISSN: 2672-7226
DOI: http://doi.org/10.46754/jssm.2026.07.010

ENVIRONMENTAL PROTECTION THROUGH IMPROVED COATING SYSTEM FOR PREVENTION OF FLOATING PRODUCTION STORAGE AND OFFLOADING SYSTEM HULL CORROSION

VINCENT O. IZIONWORU[1]*, CHARLES U. ORJI[2], WATIMIYO J. CHARLES[2], WAN MOHD NORSANI WAN NIK[3], INNOCENT O. ARUKALAM[4,5], MOHAMMAD FAKHRATUL RIDWAN ZULKIFLI[3] AND MOHAMMED ISMAIL RUSSTAM SUHRAB[3]

[1]*Department of Chemical, Petrochemical Engineering, Rivers State University, Nkpolu-Oroworukwo, Port Harcourt, Nigeria*
[2]*Department of Marine Engineering, Rivers State University, Nkpolu-Oroworukwo, Port Harcourt, Nigeria*
[3]*Faculty of Maritime Studies, Universiti Malaysia Terengganu, 21030 Kuala Nerus, Terengganu, Malaysia*
[4]*Department of Polymer and Textile Engineering, Federal University of Technology, P.M.B. 1526, Owerri, Nigeria*
[5]*Advanced Functional Materials/Corrosion Research Group, Africa Centre of Excellence in Future Energies and Electrochemical Systems (ACEFUELS), Federal University of Technology, Owerri, Nigeria*

Corresponding author: vincent.izionworu@ust.edu.ng

ARTICLE INFO

Article History:
Received: 28 April 2025
Revised: 1 May 2026
Accepted: 21 June 2026
Published: 15 July 2026

Keywords:
FPSO, corrosion, coating, epoxy, environmental pollution

ABSTRACT

Pollution of the oceanic environment in the Gulf of Guinea is a global concern, necessitating a study on the corrosion control of Floating Production Storage and Offloading systems (FPSOs) hulls exposed to an artificial metocean environment caused by heat from gas flared from flare stacks on the deck of FPSOs. This heat reduces the service life of the Standard (STD) coating system on the FPSO hull, which is designed to prevent corrosion. To avert early failure that could lead to environmental pollution and degradation, a novel coating system is formulated using a mix of epoxy paints, metals, and a unique coating sequence. Analysis of the coating system exposed to artificial metocean conditions at a maximum temperature of 96.2ºC, salinity of 33.13 ppt, and pH of 8.20, respectively, using Atomic Absorption Spectrophotometry (AAS), electrolyte absorption, and a pull test shows that the improved coating system, TY-B, showed greater stability in the electrolyte, a high pull test of 471 psi, and sustained elemental composition of zinc oxide, titanium dioxide, and aluminum oxide. The STD coating system lost more weight in the electrolyte had a lower pull test of 425 psi and had more loss of elemental composition. Compared to the STD coating system, the TY-B coating formulation is preferred for coating FPSO hulls exposed to a high-pressure gas flare system installed on the FPSO deck.

Introduction

Oil spills in the Gulf of Guinea have been attributed to factors such as vandalism, sabotage, oil production operations, pipeline and tank corrosion, and other product storage assets on offshore platforms (Najoui *et al*., 2022). Offshore platforms are huge, heavy steel, or concrete structures used in the exploration and production (extraction) of oil and gas from the Earth's crust and are designed for installation in the open sea, lakes, gulfs, etc. (Sadehgi, 2007). While the design analysis, construction of offshore structures, and magnitude of environmental pollution that can result in an ocean environment present major challenges, the range of possible designs such as Tension Leg Platforms (TLPs), deep water designs, jacket and jack-up (space truss-like) oil rigs, and ship-like floating production systems (FPSOs), pose their own peculiar demands. There are also engineering design considerations and challenges such as hydrodynamics, structural dynamics, environmental loads, and their influence (Haritos, 2007; Hwang *et al*., 2010).

Although other challenges exist such as operating conditions (location) and environmental factors outlined in API RP-2MET-INT (2012) and other relevant industry standards, including general meteorological and oceanic factors (Amaechi *et al*., 2022), FPSOs stand out as offshore structures. Unique features such as good stability and floatability have been identified to facilitate the transition, installation, and maintenance of floating production storage/offloading systems (FPSOs) (Haritos, 2007; Amaechi *et al*., 2022). FPSOs also stand out for their relatively low cost, short construction time, stability with varying payloads, and ample processing space (Zhao *et al*., 2010).

Over 270 FPSOs are successfully operating globally (Charles *et al*., 2022). They are efficient mini refineries for remote and small fields (Shimamura, 2002; Charles *et al*., 2024). Although an FPSO is made of different parts, the hull of an FPSO is one of the major parts of an FPSO (Shimamura, 2002). FPSOs are designed with a 25-year design life that covers the periods from design through commissioning, operation, and decommissioning (Stephenson, 2019).

The service life of FPSOs, like other metals and marine assets is heavily influenced by the involvement of numerous material degradation processes (such as fatigue cracking, corrosion, and pitting) as well as environmental stresses that vary with geographical locations and climatic factors (Abbas & Shafiee, 2020; Izionworu *et al*., 2025). Corrosion in FPSOs results in short- and long-term damage (Imran *et al*., 2023). Pitting stands out as an insidious, localised form of corrosion that causes severe damage to structural members such as steel, in chloride environments like electrochemical seawater (Akpanyung & Loto, 2019). In the Gulf of Guinea, FPSOs are significantly impacted by operating in high-temperature, humid, and saline marine environments that are highly corrosive (Cullum *et al*., 2018; Abbas *et al*., 2019). Also, dissolved oxygen and other species such as carbon dioxide, hydrogen sulfide, chlorides, sulfates, and various acids, as well as the metal surfaces' pH in seawater, drive electrochemical processes on the FPSO hull, resulting in massive corrosion and consequential oil spills. To manage this situation, marine corrosion maintenance strategies (Lazakis *et al*., 2016) such as Cathodic Protection (CP) and coatings are employed. Coatings can provide efficient protection over a long period of time (Ibrahim *et al*., 2020; Hossen *et al*., 2023).

A coating system that has been employed is the use of epoxy coating with different primers such as inhibitive primers, impervious primers such as Microcrystalline Cellulose (MCC) incorporated into the epoxy resin and cathodically protective primers (Zika, 2006; Ahmad *et al*., 2024). Sadly, about 3% of FPSO coatings break down within the first three years of operation. A 10ºC increase in temperature would double corrosion (Andrien, 2004; Charles *et al*., 2022; 2024). Gas flare radiation, pH, and salinity factors intensify FPSO corrosion and coating failure (Charles *et al*., 2024). There is therefore a need for an efficient coating formulation to eliminate the impact of complex interaction factors such as adhesion, application, and design-related failures (Zaki, 2006; Haque *et al*., 2023; Charles *et al*., 2024).

Consequently, this study developed an improved coating system for FPSOs to prevent environmental damage from coating failures. The research also determined the coating's protective effectiveness by analysing and characterising it using an Atomic Absorption Spectrometer (AAS) to measure its efficacy, gravimetric measurement to assess electrolyte absorption, and a pull test to check its adhesive strength. Additionally, the study determined how the coating system is affected by environmental changes around the gas flare, specifically increased radiation temperatures and artificial metocean conditions within the flare perimeter.

Materials and Methods

Materials

The materials used in this study include Testex (Press-O-Film), tanks, an Elcometer, deionised water, glassware, and a volumetric flask of suitable precision and accuracy. Solar thermo elemental Atomic Absorption Spectrophotometer (Flame AAS) mode: S4=71096, pipettes (microliters with disposable tips), and pressure-reducing valves.

The study area is the Gulf of Guinea, situated at the intersection of the equator and the prime meridian, having coordinates of 0°N and 0°E, and spanning about 2,350,000 km². The Gulf's coastline features the Bight of Benin and the Bight of Bonny [Figure 1 (a)] (Rosemberg, 2020). The Gulf of Guinea is an area rich in hydrocarbon potential and plays a crucial role in global oil markets (Onuoha, 2009). Oil and gas exploration in this area has historically utilised offshore permanent platforms with FPSOs. The electrolyte (water) was simulated to mimic the Gulf of Guinea in the Atlantic Ocean.

Methods

Sample Surface Preparation

Mild steel sheets with the composition described in Table 1 were mechanically cut to 40 mm x 120 mm x 3 mm coupons [Figure 1 (b)]. The Relative Humidity (RH), Steel Temperature (Ts), Air Temperature (Ta), and Dew Point Temperature (Td) were checked and recorded with the aid of the Elcometer to ensure recommended environmental conditions before sandblasting the coupons [Figures 2 (a) and (b)]. Also, the anchor profile of the sample coupons was recorded using the Testex (Press-O-Film) and Elcometer. The coupons were weighed and stored in a desiccator.

Preparation of Electrolyte (Sea Water)

The seawater for the study was collected from the Atlantic Ocean (Gulf of Guinea). The seawater was analysed to establish baseline pH and salinity levels, then treated in the laboratory to create high- and low-salinity concentrations and pH values representing the dry and rainy season metocean conditions in the Gulf of Guinea, as shown in Table 2.

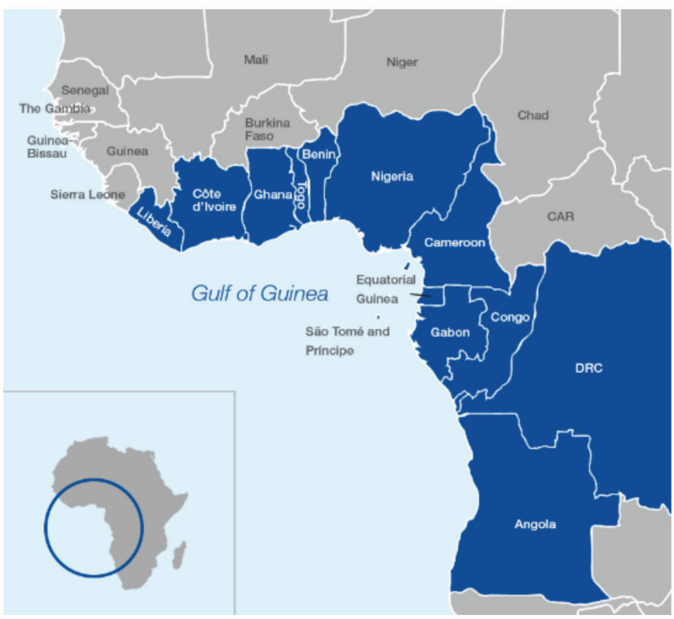

Figure 1 (a): Gulf of Guinea
Source: Institute for Security Studies (2024)

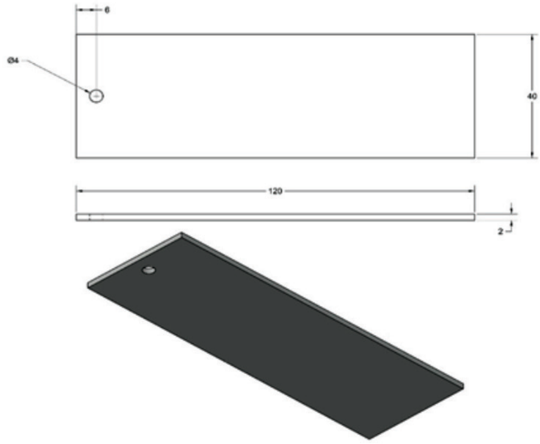

Figure 1 (b): Coupon dimension

(a)

(b)

Figure 2: Coating process of the coupons
Source: Charles (2024), field work

Table 1: Composition of mild steel

Element	Percentage Composition (%)
Carbon	0.05
Silicon	0.03
Manganese (Mn)	0.6
Phosphorus (P)	0.35
Iron (Fe)	99.51

Table 2: Simulated metocean conditions for salinity and pH of Gulf Guinea seawater

Amount of Water (l)	Salinity (ppm)		pH	
	High	Low	High	Low
750	33.13	24.03	7.50	8.20

Coating System Formulation

An existing coating system, identified as the standard coating (hereafter referred to as STD) (Table 3) and an improved coating system, identified as Type B (TY-B) were prepared. The first coat in each case is the primer in a three-stage coating system that has an intermediate and a top coat as the basic standard (Zaki, 2006). The primer in the improved coating system was composed of Zinc oxide (at 62.17% of the Metallic oxides), followed by the usual aluminium-based primer, and then a vinyl paint (Zulkifli *et al.*, 2021). The Epoxy paint has a molecular weight range of 700–1,200 and is composed of xylene, hydrocarbons, C9 aromatics, and 1-methoxy-2-propanol.

Others are ethylbenzene, hydrocarbons, C9-C12, n-alkanes, isoalkanes, cyclics, aromatics (2-25%) fatty acids, C14-18, and C16-18-unsaturated maleated. The specific paint brand and exact formulations are proprietary. A wet film thickness requirement of 75 microns and the dry film thickness requirement of 50 microns were achieved during coating [Figures 2 (a) and (b)]. The ambient temperature, wind speed, and humidity records are presented in Table 4 and Figure 3.

Experimental Setup and Procedures

Four water baths labelled Tank 1, Tank 2, Tank 3, and Tank 4, also referred to as T1, T2, T3, and T4, respectively, were filled with 75 litres of prepared electrolyte. Each tank contained the electrolyte and temperature conditions described in Table 5 and the required temperature was estimated as reported in the literature (Charles *et al*., 2024). 3 mm-diameter steel rods were used to suspend the coated coupons in the electrolyte. These allowed for immersion of the coupons into artificial metocean conditions mimicking the FPSO's peak and off-peak periods in the Gulf of Guinea (Charles *et al*., 2024). The experiment is setup as depicted in Figure 4. Each tank contained 12 standard coupons and 12 Type-B coupons, which were immersed for

Table 3: Sample 1 (Standard formulation)

Coat (Name of Paint/Colour)	Order of Coating
Marine Epoxy (Alu Based)	1st coat
Marine Epoxy (Bronze)	2nd coat
Mastic Epoxy (Aluminium)	3rd coat
Epoxy Top Coat (Off Blue)	4th coat
Epoxy Top Coat (Blue)	5th coat

Table 4: Ambient condition temperature, wind speed, and humidity

Climatic Condition in Work Area				Condition for Steel Blasting	Nozzle Pressure
Time (Hrs)	09:20	10:22	12:11	Light Mill Scale	6.5 Bar (94.25 psi)
Relative Hum. (%)	76:00	67:30	75:20		
Ambient Temp. (ºC)	28:50	31:00	30:50	✓	
Surface Temp. (ºC)	29:10	30:60	30:20		
Dew Point Temp. (ºC)	23:90	24:20	25:40		
				Type of Abrasive:	Blasting sand

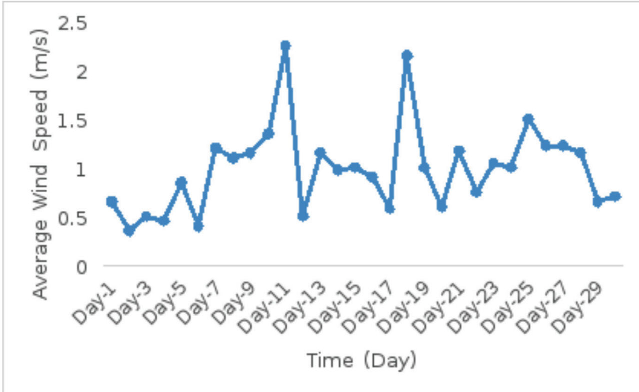

Figure 3: Wind speed profile

30 days. Temperature variation around the flare area–the water baths, sterile area zones at 12, three, six, and nine o'clock–and the centre of the sterile area and inside of it were also identified and recorded.

Coating System Exposure and Electrolyte Absorption Measurement

The already cleaned and weighed coupons were coated and reweighed, the records were kept as a baseline for gravimetric analysis. Immersion

Figure 4: Main experimental setup

Table 5: Simulated metocean conditions

Tank Type	Artificial Metocean Parameters		
	Salinity (ppm)	Temp. (ºC)	pH
1	24.03	70.0	7.50
2	33.13	96.2	8.20
3	24.03	96.2	7.50
4	33.13	70.0	8.20

test of the coated coupons in Tanks 1, 2, 3, and 4 was conducted, the coupons were weighed after withdrawal from the electrolytes every five days for 30 days. To simulate the flash zone of an FPSO, the coupons were removed from the electrolyte after two days of immersion, allowed to stand for 24 hours, re-immersed on the third day, and removed on the fifth day. Two STD-coated coupons and two TY-B-coated coupons from each of the four Tanks were collected for analysis. Weight gain or loss for each coated coupon was measured to assess electrolyte absorption using equation (1). The pull test was performed and samples were collected for Atomic Absorption Spectroscopy (AAS) analysis.

$$W_{ai} - W_{bi} = \Delta W_{g/l} \quad (1)$$

where W_{ai} is the weight of the coupon after immersion in each metocean tank; W_{bi} is the weight of each coupon before immersion, and $\Delta W_{g/l}$ represents weight gain or loss after immersion of the coupons.

Pull Test Procedure

The adhesion pull test was conducted using the Elcometer 106 Pull Off Adhesion Tester in accordance with the National and International Standards (ASTM D 4541, 2012 & ISO 4624). The Elcometer 106/1 Scale 1(0) to 3.5 N/mm² (500 psi) was used as described in the Elcometer 106 Adhesion Tester Operating Instructions (2012). The steps for the pull-off test were: (1) Selection of the area for the pull-off test. The area selected was free of grease, oil, dirt, chalking, water, protrusions, or other conditions that could interfere with the attachment of a "dolly" to the surface. (2) Abrasion of the metal surface was done with fine-grade emery paper (2000) to create a lightly roughened surface and the resulting dust was wiped off the surface.

Atomic Absorption Spectroscope (AAS)

Solar thermo elemental Atomic Absorption Spectrophotometer (Flame AAS) was used for the elemental metal analysis with the result as a report. The resulting data of active compounds in the coating system were plotted.

Results

Electrolyte Absorption Result for Improved and Existing Standard Coating Systems

Figures 5 and 6 show the electrolyte absorption trends for TY-B and STD coupons across tanks, respectively. The results reveal TY-B's low, negative absorption values (e.g., -1.53 g in T1 day 10; max +0.59 g in T4 day 10). The figures also reveal an STD coating system that showed

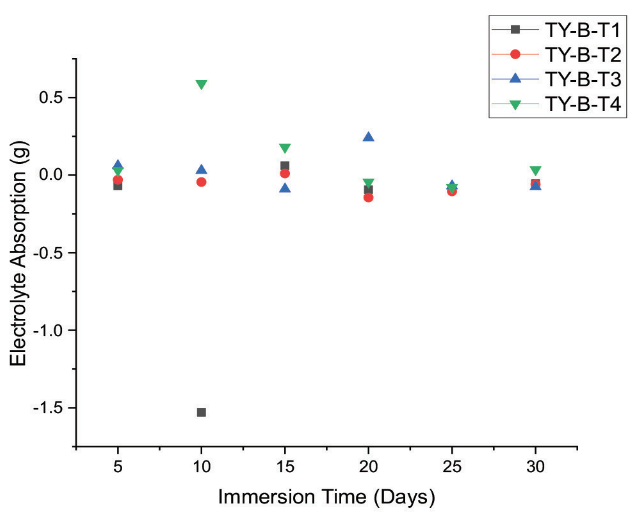

Figure 5: Electrolyte absorption trends for TY-B coupons across tanks

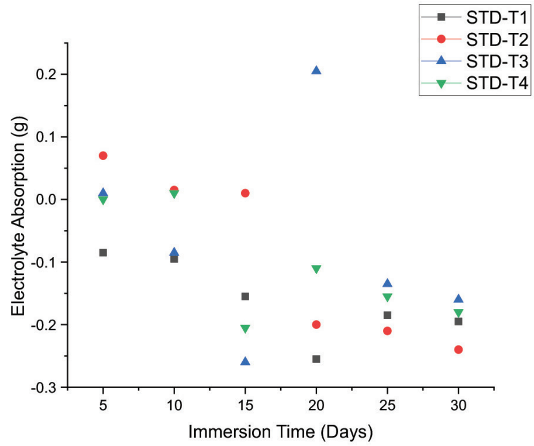

Figure 6: Electrolyte absorption trends for STD coupons across tanks

consistent negative electrolyte absorption (e.g., -0.255 g in T1 day 20), with a few positives, such as +0.205 g in T3 day 20.

Pull Test Result for Improved and Existing Standard Coating Systems

The results of the pull test for STD and TY-B coatings exposed to the treatment conditions under different metocean (temperature, salinity, and pH) conditions are shown in Figure 7. It reveals that the TY-B coating system had a pull-test strength that ranged from 350 to 475 psi against STD's 290 to 425 psi in T2, the artificial metocean with the harshest condition mimicking a dry season with higher salinity (33.13 ppm), higher pH (8.20), and the highest temperature (96.2ºC) from the flared gas. It was also observed that as immersion time increased from five to 25 days, TY-B showed higher pull-test strength.

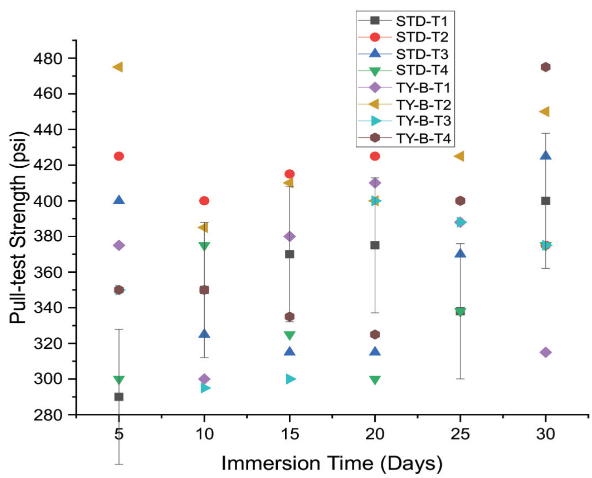

Figure 7: Pull test plots of STD and TY-B coating formulation after 30 days of immersion in T1 (lower salinity – 24.03 ppm, lower temperature – 70ºC, lower pH – 7.50), T2 (high salinity – 33.13 ppm, high temperature – 96.2ºC, high pH – 8.20), T3 (lower salinity – 24.03 ppm, high temperature – 96.2ºC, lower pH – 7.50), and T4 (high salinity – 33.13 ppm, lower temperature – 70ºC and high pH 8.20) electrolytic composition

Five days later, the better performance of TY-B pull-test strength was sustained in only T2 and T4 metocean conditions.

AAS Analysis Result for Improved and Existing Standard Coating Systems

Figure 8 presents the 30-day immersion period AAS test results on the effect of the different artificial metocean conditions on aluminium, titanium, and zinc components for STD and TY-B coating formulations and their corrosion product–Aluminium oxide (Al_2O_3), Titanium dioxide (TiO_2), and Zinc oxide (ZnO). Figure 9 shows the effect on all three compounds in T2, the harshest artificial metocean condition, with higher salinity (S), temperature (T), and pH over the 30-day immersion period. As observed in Figures 8 and 9, the AAS data show sacrificial oxide declines: TY-B Al_2O_3 (62.17% to 26.82%) in Figure 8 (a); TiO_2 (4.52% to 2.36%) seen in Figure 8 (b); ZnO (62.17% to 26.82%) seen in Figure 8 (c); STD Al_2O_3 (10.25% to 7.51%) presented in plots of Figure 8 (a), TiO_2 (6.71% to 4.83%) presented in Figure 8 (b), and ZnO (79.39% to 65.48%) as seen in Figure 8 (c).

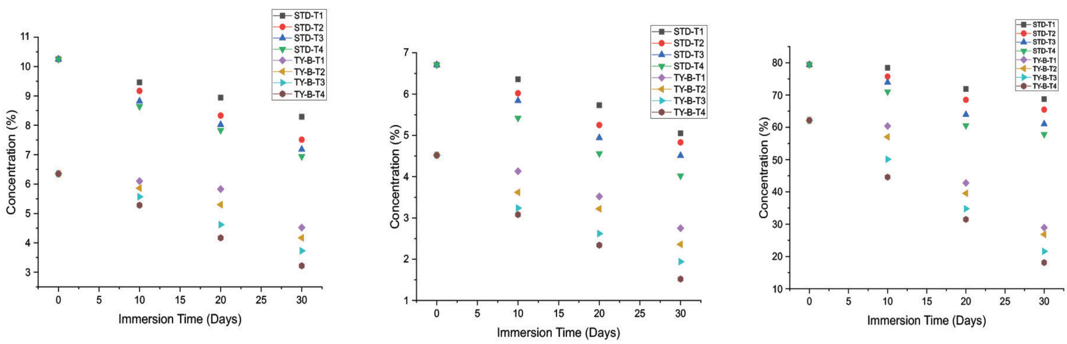

(a) (b) (c)

Figure 8: Concentration of (a) aluminium oxide, (b) titanium dioxide, (c) zinc oxide components of STD and TY-B coating systems in artificial metocean conditions of T1, T2, T3, and T4 over a 30-day immersion period

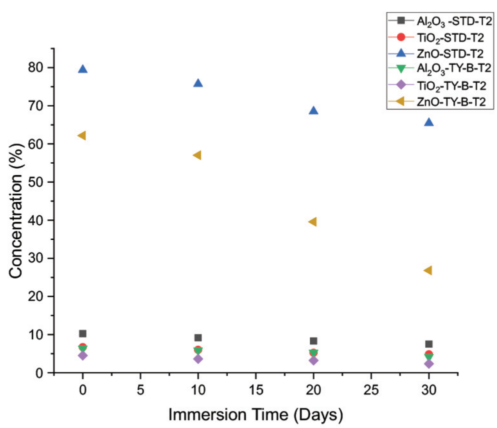

Figure 9: Concentration of aluminium oxide, titanium dioxide, and zinc oxide components of STD and TY-B coating system in artificial metocean conditions of T2 (high salinity – 33.13 ppm, high temperature – 96.2ºC, and high pH – 8.20), over a 30-day immersion period

Discussion

The results of Figures 5 and 6 reveal TY-B's robust barrier with limiting electrolyte ingress across T1-T4 despite salinity, temperature, and pH variations. This outcome can be traced to TY-B's denser coating polymer matrix, which is seen to excel in harsh T2 conditions (high salinity, temperature, and pH). This improved chemical stability reduced diffusion pathways, thereby improving the performance of the TY-B coating system. A different trend is observed for the STD coating system.

The negative absorption values at 30 days for STD across T1–T3 indicate possible thermal degradation, leaching, or thickness-related loss mechanisms. These are attributed to the release of volatile degradation products or to solvent evaporation from the coating matrix under harsh environmental stresses, caused by the extreme artificial metocean condition, with the greatest effect at higher temperature and pH in T2 (Xian *et al*., 2024; Zargarnezhad *et al*., 2021). A plausible implication of the observed electrolyte absorption by the STD coating system in T3 is increased ion permeability, leading to corrosion under high-temperature, low-pH stress (Senderowski *et al*., 2024). This mechanism explains why STD coatings are exposed to shrinkage and breakage.

The results confirm that the newly formulated TY-B coating system offers significantly enhanced protective efficacy and durability compared to the STD coating system, particularly under aggressive metocean conditions. This is substantiated by the sustained high pull-test strength observed in T2 and T4 environments, characterised by high temperatures, high salinity, and pH, which provide compelling evidence of TY-B's superior performance. This resilience is noteworthy, as high temperatures and high salinity are known to accelerate coating degradation (Chohan *et al*., 2024: Shi *et al*., 2025) and corrosion rates by enhancing the kinetic energy of degradation processes.

The fundamental basis for TY-B's superior mechanical performance lies in its formulation. The design successfully achieved a higher crosslinking density and established a tight, three-dimensional epoxy polymer network within the coating matrix. The epoxy polymer heteroatoms–Oxygen (O), Nitrogen (N) from the hardener, and the epoxide group (also known as a glycidyl group or oxirane ring) may have formed dative covalent bonds with the surface of the substrate (Liang *et al*., 2024). This structure was specifically engineered to improve thermal resistance, as confirmed by the system's ability to maintain pull-off strength after exposure to 96.2°C. This stability successfully counteracted the potential for thermal softening and a subsequent viscoelastic creep that may have compromised the STD system's integrity, leading to a decrease in the material's glass transition temperature.

Beyond mechanical stability, the TY-B system exhibited improved barrier properties. The low diffusion observed for the electrolyte containing aggressive species (Cl^{-1} and OH^{-1} ions) (Liang *et al*., 2024) highlights the effectiveness of the epoxy polymer composition in hindering mass transport. This enhanced chemical barrier function slowed the ingress of corrosive species, preventing hydrolytic destabilisation and mitigating competition between water molecules and the polymer for bonding sites at the substrate interface.

In essence, the TY-B coating protects through a synergistic dual-mechanism, combining its intrinsically strong polymer network inherent in epoxies with a chemically resistant adhesive interface. This combination successfully preserved the critical chemical and mechanical interlocking forces, preventing potential for corrosion action on the surface of the substrate as reported by Senderowski *et al*. (2024). It also prevented delamination and established TY-B as a robust alternative to the current STD coating in demanding service environments.

In addition, the decreases in the sacrificial oxides observed in Figures 8 and 9 were expected (Dagdag *et al*., 2020) and likely indicate sacrificial corrosion protecting the substrate. This is consistent with the reports of Kumar *et al*. (2002), Brostow *et al*. (2010), and Mirzakhanzadeh *et al*. (2018) that the corrosion product ZnO contributes to the corrosion-prevention capacity of coatings (Meng *et al*., 2019). It has also been reported that increasing the zinc powder content in an epoxy coating by 25% results in excellent corrosion protection for the substrate. So, Zinc oxide in both STD and TY-B coatings acts as a sacrificial anode, forming protective zinc carbonate layers that offer corrosion resistance in high saline, high-pH, and elevated temperature environments (Mirzakhanzadeh *et al*., 2018; Meng *et al*., 2019; Smit *et al*., 2020; Senderowski *et al*., 2024).

Of particular interest is the importance of Zinc Nanoparticles (Zn NPs) used in the coatings. The Zn NPs exhibit behaviour sensitive to pH and salinity. It has been reported that at high salinity, Zn NPs promote aggregation reducing dispersibility while alkaline pH, like acid pH, enhances dissolution releasing Zn^{2+} ions (Smit *et al*., 2020: Senderowski *et al*., 2024). This results in slower degradation and better long-term corrosion inhibition compared to STD coatings. ZnO further provides UV protection, minimising polymer breakdown, especially at 96.2°C in the presence of sunlight, thereby extending coating lifespan.

Another sacrificial oxide aluminium oxide (Al_2O_3) contributes a hard, chemically resilient barrier in both coatings, resisting chloride (Cl^{-1}) and hydroxide (OH^{-1}) ions prevalent in seawater (Liang *et al*., 2024) while affording excellent thermal shock resistance. However, TY-B appears to have a denser or more augmented Al_2O_3 (i.e., the amphoteric oxide) layer, which sustains coating adhesion and minimises microcracking under thermal gradients in Tanks 2 and 3. The amphoteric oxide layer protects the coating across the pH ranges in the tanks by limiting localised corrosion and substrate dissolution. This results in enhanced mechanical stability and durability compared to STD coatings.

TY-B's lower TiO_2 concentration as seen in the plots of Figure 8 (b) across tanks exposed to elevated temperatures, combined with optimised distribution, delivers superior UV protection and corrosion resistance compared to STD. TY-B achieves this by reducing coating degradation and metal ion penetration. Again, because TiO_2's crystalline hardness improves film toughness against erosion, TY-B offers abrasion resistance, which is critical in turbulent marine conditions that the coating will be exposed.

As established above, ZnO nanoparticles in saline environments can partially dissolve to release Zn^{2+} ions (Smit *et al*., 2020; Senderowski *et al*., 2024), with the potential to cause oxidative stress and sublethal effects in aquatic organisms, especially at elevated concentrations or under low pH and low salinity conditions; it is worthy of note that, their actual ecotoxicity is strongly controlled by aggregation, surface coating, and matrix immobilisation conferred by the polymer matrix (Asiri *et al*., 2024; Hazeem, 2022).

Again, nanoparticles of Al_2O_3 and TiO_2 may induce oxidative stress or act as persistent particulates, particularly under photoactivation (TiO_2) or at high loading levels, even though they are somewhat insoluble; their risk is reduced when they are not freely dispersed in water but bound within a polymer matrix with low solubility. In the present system, the ZnO, TiO_2, and Al_2O_3 nanoparticles are incorporated at low loadings and are immobilised within the epoxybased coating of TY-B coating system, limiting their leaching and bioavailability in seawater while retaining their protective function; this "safetybydesign" approach is intended to mitigate corrosionrelated emissions and maintenance impacts without introducing a new marine pollutant, though quantitative release and ecotoxicity testing under realistic marine conditions would further validate this environmental safety claim.

Conclusions

This study demonstrates that the TY-B coating system outperforms the standard STD coating system in protecting FPSO hulls against corrosion under various harsh artificial metocean conditions. The enhanced coating's effectiveness stems from the synergistic interaction of its constituents–aluminium oxide, titanium oxide, zinc oxide, and an epoxy polymer–which provide a tough barrier against high salinity, temperature, and pH. By minimising electrolyte absorption and improving adhesion, TY-B offers greater durability and corrosion resistance, suggesting a more sustainable approach to FPSO maintenance that could reduce environmental risks, such as oil spills. Additionally, the findings underscore the urgent need for stricter global regulations to eliminate gas flaring in related oil and gas operations, safeguarding the marine environment and the blue economy dependent on ocean resources. This comprehensive approach not only improves FPSO operational integrity but also promotes environmental stewardship.

Acknowledgements

The authors would like to acknowledge the RSU-UMT-UKM MG1+2 corrosion collaboration.

Author Contributions Statement

Vincent O. Izionworu, Charles U. Orji, and Watimiyo J. Charles carried out the research and wrote the article. Vincent O. Izionworu, Watimiyo J. Charles, and Charles U. Orji conceptualised the central research idea, and provided the theoretical framework with suggestions from Wan Mohd Norsani Wan Nik and Innocent O. Arukalam. Wan Mohd Norsani Wan Nik, Innocent O. Arukalam, Mohammad Fakhratul Ridwan Zulkifli, and Mohammed Ismail Russtam Suhrab anchored the review and revised the article. Vincent O. Izionworu and Wan Mohd Norsani Wan Nik performed final review and formatted the article for submission.

Conflict of Interest Statement

The authors agree that this research was conducted in the absence of any self-benefit, commercial, or financial conflicts and declare that there are no conflicts of interest with the funders.

References

Abbas, M., & Shafiee, M. (2020). An overview of maintenance management strategies for corroded steel structures in extreme marine environments. *Marine Structures*, *71*, 102718. https://doi.org/10.1016/j.marstruc.2020.102718

Ahmad, Z. (2006). *Principles of corrosion engineering and corrosion control*. Elsevier. https://doi.org/10.1016/B978-0-7506-5924-6.X5000-4

Ahmad, Z., Kamsani, D. M., Sin, A. L., Aziz, A. A., Yahya, S., & Shaari, H. A. H. (2024). Characterisation and density functional theory study of epoxy–microcrystalline cellulose primer coating. *Iranian Polymer Journal*, *34*, 841–852. https://doi.org/10.1007/s13726-024-01409-3

Akpanyung, K. V., & Loto, R. T. (2019). Pitting corrosion evaluation: A review. *Journal of Physics: Conference Series*, *1378*(2), 022088. https://doi.org/10.1088/1742-6596/1378/2/ 022088

Amaechi, C. V., Chesterton, C., Butler, H. O., Gillet, N., Wang, C., Ja'e, I. A., Reda, A., & Odijie, A. C. (2022). Review of composite marine risers for deep-water applications: Design, development and mechanics. *Journal of Composites Science*, *6*(3), 96. https://doi.org/10.3390/jcs6030096

American Petroleum Institute. (2012). *API RP 2MET—Derivation of metocean design and operating conditions*.

American Society for Testing and Materials. (2022). *Standard test method for pull-off strength of coatings using portable adhesion* *testers* (ASTM D4541-22). https://doi.org/10.1520/D4541-22

Asiri, A. M., Pugliese, V., Coppola, G., Khan, S. B., Alamry, K. A., Alfifi, S. Y., Marwani, H. M., Alotaibi, M. M., Petrosino, F., & Chakraborty, S. (2024). Zinc oxide nanoparticles immobilized on polymeric porous matrix for water remediation. *Emergent Materials*, *7*(4), 1531–1544. https://doi.org/10.1007/s42247-024-00728-8

Brostow, W., Dutta, M., & Rusek, P. (2010). Modified epoxy coatings on mild steel: Tribology and surface energy. *European Polymer Journal*, *46*(11), 2181–2189. https://doi.org/10.1016/j.eurpolymj.2010.08.006

Caralb News. (2021). *What are the types of different offshore platforms*. Caralb News. https://www.caralb.com/2021/05/31/offshore-platforms/

Charles, J. W., Izionworu, V. O., & Orji, C. (2024). Estimating flare gas heat radiation temperature and its effect on FPSO hull corrosion in the Gulf of Guinea. *Journal of Newviews in Engineering and Technology*, *6*(1), 1–16.

Charles, W. J., Izionworu, V. O., & Orji, C. U. (2022). FPSO hull corrosion management to minimize operational down-time due to artificial metocean conditions: A thermal approach. *Proceedings of the International Conference on Newviews in Engineering and Technology Maiden Edition*, 228–241.

Chohan, I. M., Ahmad, A., Sallih, N., Bheel, N., Salilew, W. M., & Almaliki, A. H. (2024). Effect of seawater salinity, pH, and temperature on external corrosion behavior and microhardness of offshore oil and gas pipeline: RSM modelling and optimization. *Scientific Reports*, *14*(1), 16543. https://doi.org/10.1038/s41598-024-67463-2

Cullum, J., Binns, J., Lonsdale, M., Abbassi, R., & Garaniya, V. (2018). Risk-based maintenance scheduling with application to naval vessels and ship. *Ocean Engineering*, *148*, 476–485. https://doi.org/10.1016/j.oceaneng.2017.11.044

Dagdag, O., Berisha, A., Safi, Z. S., Dagdag, S., Berrani, M., Jodeh, S., Verma, C., Ebenso, E., Wazzan, N., & Elharfi, A. (2020). Highly durable macromolecular epoxy resin as anticorrosive coating material for carbon steel in 3% NaCl: Computational supported experimental studies. *Journal of Applied Polymer Science*, *137*(34), 49003. https://doi.org/10.1002/app.49003

Elcometer. (2012). *Elcometer 106 adhesion tester operating instructions* (Doc. No. TMA-0003 Issue 09).

Eliboev, I., Berdimurodov, E., Yakhshinorov, K., Abdisattarov, J., Dagdag, O., Berisha, A., Wan Nik, W. B., Kholikov, A., Akbarov, K. (2023). Supramolecular corrosion protection: Eco-friendly synthesis and efficacy of a β-cyclodextrin/o-phenylenediamine complex. *Journal of the Taiwan Institute of Chemical Engineers*, *147*(6), 104944. https://doi.org/10. 1016/j.jtice.2023.104944

Haque, J., Saleh, T. A., Murmu, M., Chauhan, D. S., Nik, W. W., Banerjee, P., & Quraishi, M. A. (2023). Synthesis of multi donating sites grafted on graphene oxide nanosheets: Anti-corrosion study for mild steel in 1M HCl with DFT calculations. *Journal of Molecular Liquids*, *389*, 122820. https://doi.org/10.1016/j.molliq.2023.122820

Haque, J., Zulkifli, M. F. R., Ismail, N., Quraishi, M. A., Ghazali, M. S. M., Berdimurodov, E., & Wan Nik, W. N. N. (2023). Environmentally benign water-soluble sodium L2-(1-Imidazolyl) alkanoic acids as new corrosion inhibitors for mild steel in artificial seawater. *ACS Omega*, *8*(28), 24797–24812. https://doi.org/10.1021/acsomega. 3c00366

Haritos, N. (2007). Introduction to the analysis and design of offshore structures—An overview. *Electronic Journal of Structural Engineering*, *7*(1), 55–65. https://ejsei.com/EJSE/article/download/65/64

Hart, H. I. (2018). *Sustainable electricity generation in Nigeria: Of enthalpy, entropy, exergy and all that, not politics* [Inaugural lecture]. Rivers State University.

Hazeem, L. (2022). Single and combined toxicity effects of zinc oxide nanoparticles: Uptake and accumulation in marine microalgae, toxicity mechanisms, and their fate in the marine environment. *Water*, *14*(17), 2669. https://doi.org/10.3390/w14172669

Hossen, A., Rashel, K. M., Islam, A., Ahsan, S. K., & Mondal, M. I. H. (2023). Minimization of corrosion in aquatic environment – A review. *International Journal of Hydrology*, *7*(1), 9–16. https://medcraveonline.com/IJH/IJH-07-00334.pdf

Hwang, J. K., Roh, M. I., & Lee, K. Y. (2010). Detailed design and construction of the hull of a floating, production, storage and off-loading (FPSO) unit. *Ships and Offshore Structures*, *5*(2), 93–104. https://doi.org/10.1080/17445300903169168

Ibrahim, N. F., WanAbdullah, W. R., Rooshde, M. S., Mohd-Ghazali, M. S., & Mohd-Norsani, W. N. W. (2020). Corrosion inhibition properties of epoxy-zinc oxide nanocomposite coating on stainless steel 316L. *Solid State Phenomena*, *307*, 285–290. https://doi.org/10.4028/www.scientific.net/SSP.307.285

Ikhmal, W. M. K., Yasmin, M. Y. N., Fazira, M. F. M., Rafizah, W. A., Wan-Nik, W. B., & Sabri, M. G. M. (2017). Anticorrosion coating using *Olea* sp. leaves extract. *IOP Conference Series: Materials Science and Engineering*, *344*, 012028. https://doi.org/10.1088/1757-899X/344/1/012028

International Organization for Standardization. (2023). *Paints and varnishes — Pull-off test for adhesion* (ISO 4624:2023).

Izionworu, V. O., Byadi, S., Arukalam, I. O., & Nik, W. M. N. W. (2022). Inhibitive mechanism of acid corrosion of cold-rolled steel by polyethylene glycol via experimental, computational and surface analytical approaches. *Journal of Bio- and Tribo-Corrosion*, *8*(14), 1–14. https://doi.org/10.1007/s40735-021-00613-5

Izionworu, V. O., Oguzie, E. E., & Amadi, S. A. (2020). Electrochemical, SEM, GC-MS and FTIR study of inhibitory property of cold extract of *Theobroma cacao* pods for mild steel corrosion in hydrochloric acid. *International Journal of Engineering Trends and Technology*, *68*(2), 82–87. https://doi.org/10.14445/22315381/IJETT-V68I2P214

Izionworu, V. O., Oguzie, E. E., & Arukalam, O. I. (2020). Thermodynamic and adsorption evaluation of *Codiaeum variegatum brilliantissima* - Zanzibar as inhibitor of mild steel corrosion in 1 M HCl. *Journal of Newviews in Engineering and Technology*, *2*(4), 1–13. https://repository.futo.edu.ng/handle/20.500. 14562/1402

Izionworu, V. O., Puyate, Y. T., & Wan-Nik, W. M. N. (2021). A study of wire croton as an inhibitor of mild steel in HCL using electrochemical – SEM – GCMS and FTIR measurements. *Journal of Newviews in Engineering and Technology*, *3*(1), 1–11.

Izionworu, V. O., Ukpaka, C. P., & Oguzie, E. E. (2020). Inhibition of mild steel corrosion in acidic medium using *Theobroma cacao* pod. *International Journal of Scientific & Engineering Research*, *11*(3), 255–256. https://repository.futo.edu.ng/handle/20.500.14562/1408

Izionworu, V. O., Wan-Nik, W. B., Chuku, J., Amadi, C., Okparanma, R. N., & Ehirim, E. O. (2025). Vandalism-induced corrosion: A review of oil and gas facility protection options. *Journal of Newviews in Engineering and Technology*, *7*(1), 131–142.

Jeon, J. M., Yoo, Y. R., Jeong, M. J., Kim, Y. C., & Kim, Y. S. (2021). Effect of solution temperature on the cavitation degradation properties of epoxy coatings for seawater piping. *Corrosion Science and Technology*, *20*(6), 335–346. http://doi.org/10.14773/cst.2021.20.6.335

Kumar, S. A., Alagar, M., & Mohan, V. (2002). Studies on corrosion-resistant behavior of siliconized epoxy interpenetrating coatings over mild steel surface by electrochemical methods. *Journal of Materials Engineering and Performance*, *11*(2), 123–129. https://doi.org/10.1361/105994902770344178

Lamghafri, S., Daoudi, W., Dagdag, O., Naguib, I. A., Wan Nik, W. N. N., Berisha, A., Kim, H., El Aatioui, A., Zarrouk, A., & Lamhamdi, A. (2025). Promising corrosion resistance of mild steel, copper, and aluminum in hydrochloric acid solution using an environmentally friendly corrosion inhibitor. *Journal of Industrial and Engineering Chemistry*, *146*, 332–348. https://doi.org/10.1016/j.jiec.2024.11.016

Lazakis, I., Dikis, K., Michala, A. L., & Theotokatos, G. (2016). Advanced ship systems condition monitoring for enhanced inspection, maintenance and decision making in ship operations. *Transportation Research Procedia*, *14*, 1679–1688. https://doi.org/10.1016/j.trpro. 2016.05.133

Liang, H., Shi, X., & Li, Y. (2024). Technologies in marine antifouling and anti-corrosion coatings: A comprehensive review. *Coatings*, *14*(12), 1487. https://doi.org/10.3390/coatings14121487

MacMillan, A., Fischer, K. P., Carlsen, H., & Goksoyr, O. (2004). Newbuild FPSO corrosion protection – A design and operation planning guideline. *Offshore Technology Conference*, 1–11. https://doi.org/10.4043/16048-MS

Meng, Y., Liu, L., Zhang, D., Dong, C., Yan, Y., Volinsky, A. A., & Wang, L. N. (2019). Initial formation of corrosion products on pure zinc in saline solution. *Bioactive Materials*, *4*, 87–96. https://doi.org/10.1016/j.bioactmat.2018.08.003

Mirzakhanzadeh, Z., Kosari, A., Moayed, M. H., Naderi, R., Taheri, P., & Mol, J. M. C. (2018). Enhanced corrosion protection of mild steel by the synergetic effect of zinc aluminum polyphosphate and 2-mercaptobenzimidazole inhibitors incorporated in epoxy-polyamide coatings. *Corrosion Science*, *138*, 372–379. https://doi.org/10.1016/j.corsci.2018.04.040

Najoui, Z., Amoussou, N., Riazanoff, S., Aurel, G., & Frappart, F. (2022). Oil slicks in the Gulf of Guinea–10 years of Envisat advanced synthetic aperture radar observations. *Earth System Science Data*, *14*(10), 4569–4588. https://doi.org/10.5194/essd-14-4569-2022

National Institute of Standards and Technology. (2023). *NIST/EPA/NIH mass spectral library 2023*. https://sciencesolutions.wiley.com/wp-content/uploads/2025/07/NIST-EPA-NIH-Mass-Spectral-Library-Datasheet.pdf

Onuoha, G. (2009). Energy and security in the Gulf of Guinea: A Nigerian perspective. *South African Journal of International Affairs*, *16*(2), 245–264. https://doi.org/10.1080/10220460903269008

Rosenberg, M. (2020). *Where do the Prime Meridian and the Equator intersect?* ThoughtCo. https://www.thoughtco.com/prime-meridian-and-the-equator-intersect-4070819

Sadeghi, K. (2007). An overview of design, analysis, construction and installation of offshore petroleum platforms suitable for Cyprus oil/gas fields. *Girne American University Journal of Social and Applied Science*, *2*(4), 1–16. https://cemtelecoms.iqpc.co.uk/media/6514/786.pdf

Senderowski, C., Rejmer, W., Vigilianska, N., & Jeznach, A. (2024). Changes in corrosion behaviour of zinc and aluminium coatings with increasing seawater acidification. *Materials*, *17*(3), 536. https://doi.org/10.3390/ma17030536

Shi, X., Kong, W., Cheng, G., & Sun, Y. (2025). Research on corrosion status of FPSO pipeline network material and countermeasures. In *ISOPE International Ocean and Polar Engineering Conference*. ISOPE. https://onepetro.org/ISOPEIOPEC/proceedings-abstract/ISOPE25/ISOPE25/ISOPE-I-25-481/713083

Shimamura, Y. (2002). FPSO/FSO: State of the art. *Journal of Marine Science and Technology*, *7*(2), 59–70. https://doi.org/10.1007/s007730200013

Smith, F., Brownlie, F., Hodgkiess, T., Toumpis, A., Pearson, A., & Galloway, A. M. (2020). Effect of salinity on the corrosive wear behaviour of engineering steels in aqueous solutions. *Wear*, *462*, 203515. https://doi.org/10.1016/j.wear.2020. 203515

Stephenson, H. (2019). *FPSO design life*. https://www.offshoreenergylaw.com/sites/default/files/pdf/FPSO%20design%20life_new%20banner.pdf

Xian, G., Wang, Z., Kong, D., Dong, S., Li, C., & Hong, B. (2024). Degradation of an underwater epoxy adhesive and its bonding to steel subjected to water or seawater immersion. *International Journal of Adhesion and Adhesives*, *132*, 103711. https://doi.org/10.1016/j.ijadhadh.2024.103711

Zargarnezhad, H., Asselin, E., Wong, D., & Lam, C. C. (2021). A critical review of the time-dependent performance of polymeric pipeline coatings: Focus on hydration of epoxy-based coatings. *Polymers*, *13*(9), 1517. https://doi.org/10.3390/polym13091517

Zhao, L., Cui, C., Wang, Q., & Bu, S. (2010). Growth characteristics and corrosion resistance of micro-arc oxidation coating on pure magnesium for biomedical applications. *Corrosion Science*, *52*(7), 2228–2234. https://doi.org/10.1016/j.corsci.2010.03.008

Zulkifli, M. F. R., Shamsul, B. S. N., Abdullah, S., Ghazali, M. S., & Wan, W. M. N. (2021). *Citrus aurantifolia* leaf extract as a potential anti-corrosion additive in alkyd paint for mild steel. *Journal of Sustainability Science and Management*, *16*(3), 10–20. https://doi.org/10.46754/jssm.2021.04.002